固定プリントヘッドアレイ構造において発生したプリント不均一性を補償するための，完全自動化されたキャリブレーション手順

Fully Automated Calibration Procedure to Compensate Print Non-Uniformities Incurred in Fixed Print-Head Array Structures

スリーナス・ラオ ヴァントラム* カティーク チャンドゥ** マイケル スタニッチ** ラリー アーンスト**
Sreenath Rao VANTRAM Kartheek CHANDU Mikel STANICH Larry ERNST

要 旨

本稿では，CMYKインクジェットプリンタの出力不均一性を補正する，自動化されたソリューションを提案する．このソリューションは，固定プリントヘッドアレイを用いたプリンタに適用される．アルゴリズムは最初に，所望の関心領域（ROI）を分離するための印刷出力のスキャン画像を前処理する．ROI情報は，印刷領域全体にわたって不均一性を抽出するために利用される．最後に，アルゴリズムは，識別された不均一性の補償を可能にし，所望の階調応答を提供する較正ステップで終了する．

ABSTRACT

In this paper we propose an automated solution that compensates for CMYK inkjet printer output non-uniformities. The solution is applied to a printer employing fixed printhead arrays. The algorithm initially pre-processes scanned image of printed output to isolate the desired region of interest. The region of interest information is utilized to extract non-uniformities across the entire printed area. Finally, the algorithm concludes in a calibration step that enables compensation of the identified non-uniformities and provides the desired tonal target response.

* リコープロダクションプリントソリューションズLLCの夏季インターンシップ（2008年から2011年）
A summer intern (2008-2011) of Ricoh Production Print Solutions LLC

** リコープロダクションプリントソリューションズLLC
Ricoh Production Print Solutions LLC

1. Introduction

Current high speed inkjet printers commonly employ fixed-array printheads. Fixed-array systems are constructed from multiple printhead modules combined together edge-to-edge, each comprised of several hundred nozzles ejecting ink onto the media/paper. The array remains stationary while the media/paper moves across the heads, creating a process capable of printing at thousands of feet per minute.

At the same time, these fixed-array printhead systems produce inherent print artifacts. The artifacts addressed in this paper include printhead overlaps, variations between printheads and variations between nozzles. Overlaps occur due to redundant nozzles from adjacent printhead modules printing the same data, so as to avoid printing gaps. The amount of ejected ink can vary on a macroscopic level between different printhead modules and microscopically for each nozzle. Figure 1 illustrates these artifacts. A clogged nozzle is a common inkjet failure mechanism, caused by drying of ink in the nozzle, accumulated paper dust at the nozzle plate, increase in ink viscosity, and intrusion of air bubbles. Clogged nozzles results in a rapidly decreasing mean OD, and a partially clogged nozzle results in deviated ink drop producing a negative OD transition adjacent to a positive transition, as shown in Fig.1.

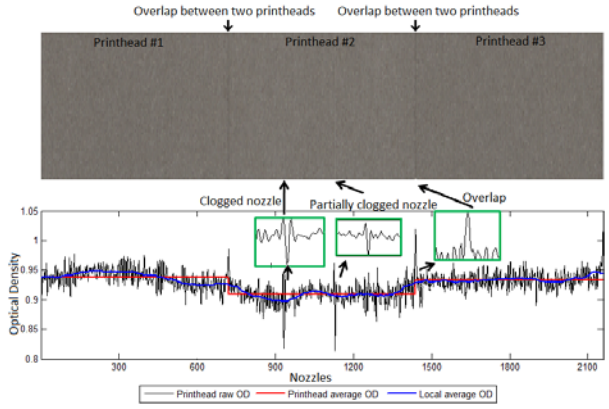

Fig.1 Illustration of artifacts incurred in a fixed-array printhead system.

After a thorough literature search, it is our view that most of the automatic print inspection and calibration systems have been developed in-house by manufactures or third party vendors for specific applications and not published in scientific literature. Automatic systems, which utilize in-line scanners to compensate for print artifacts and perform calibration for high-speed fixed printhead array inkjet printers, were not found in the search. Automatic print defect detection systems[1,2], proposed in the past employing in-line scanners, only report defect information back to the system/operator.

The system we are proposing compensates for the identified defects and also calibrates the tonal response. Creating uniform Optical Density (OD) across the web for each constant tint is our objective, by making the average ejected ink constant. Calibration is employed to produce visually distinct gray levels for the entire tonal range, matched to a pre-defined target, while compensation addresses print irregularities. This paper describes an automated calibration and compensation process to reduce non-uniformities to a level where the printed output is perceived as uniform.

2. Proposed Calibration Algorithm

The proposed automated algorithm provides a robust, ink and paper independent, solution for calibrating tone levels and compensating print non-uniformities. Compensation in this fixed printhead array arrangement accounts for 1) printhead overlaps, 2) inter printhead variations, and 3) between printhead variations.

The proposed calibration process uses a pre-defined functional description of the OD target to achieve consistent output for the entire printhead array over the entire tone range. It creates a calibrated halftone mask for each color plane generated to achieve the pre-defined target response. An initial un-calibrated multi-bit stochastic halftone mask[3] is modified to account for the

non-uniformities and to achieve the pre-defined gray scale calibration response. The process considers the Point Spread Function (PSF) of the printer/inline scanner "system".

Figure 2 illustrates a high-level flowchart of the proposed process. The initial input is a scanned image of a printed step target, using the initial un-calibrated halftone for the color to be calibrated. The proposed algorithm is repeated for each of the inks/colors used in the printer. The proposed algorithm is implemented in three different modules as shown in Fig.2. The following sub-sections describe the basis and processing in each of the three modules. Ultimately a calibrated halftone threshold array is generated for each color that includes compensation at the nozzle level.

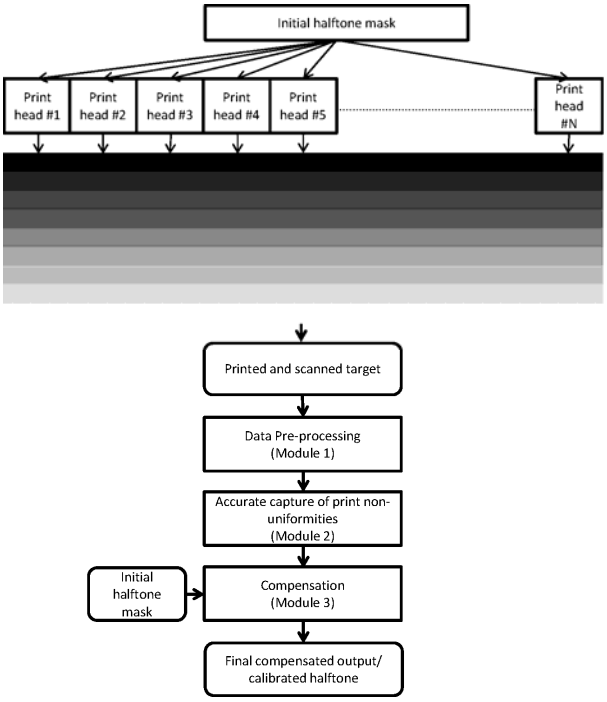

Fig.2 Proposed algorithm flowchart.

2-1 Data Pre-Processing

Module 1, labeled as the 'Data Pre-processing' in Fig.2, is responsible for: 1) extracting the portion of the printed and scanned target to be processed, 2) differentiating between tints of the step chart for each color and 3) performing image preprocessing operations such as rotation/skew, removal of unwanted regions, etc.

2-2 Accurate Capture of Print Non-Uniformities

Module 2 determines the mean OD non-uniformities for each color and tint across the entire paper web. Processing in this module includes a characterization of the PSF for the system.

2-2-1 Point Spread Function Calculation

The PSF includes the overall behavior of the printing system, including the process of scanning, which facilitates a robust solution that is independent of the machine, ink, and paper.

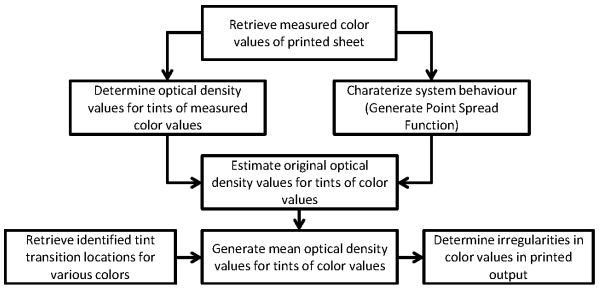

Fig.3 Accurate capture of print non-uniformities flowchart.

The PSF approach assumes a linear and shift invariant process that combines the marking process and blurring effects of the scanner optical system. In the case of an optical system, the PSF the light distribution formed at the image plane from a single point object. In our case we employ a combined PSF that provides a characterization of the printing system, print medium, and scanner. Given an input $f(x,y)$ to the printing system and its PSF $h(x,y)$, the output of the scanner $g(x,y)$, defined by Eq.1, can be mathematically computed as a two dimensional (2-D) convolution of the input $f(x,y)$ with the PSF $h(x,y)$.

$$g(x,y) = f(x,y) ** h(x,y)$$
$$= \int_{-\infty}^{+\infty}\int_{-\infty}^{+\infty} f(\alpha,\beta)h(x-\alpha.y-\beta)d\alpha d\beta, \qquad (1)$$

where α and β represent displacements of $h(x,y)$ along the horizontal and vertical spatial dimensions. The PSF can be determined by computing a Line Spread Function (LSF) derived from a line target at different orientations. If the PSF is assumed to be circularly symmetric, then the LSF at a single orientation is sufficient to derive the 2-D PSF. Experimentally the LSF, based on a single PEL width printed line, is Gaussian in our case. Consequently, we modeled the LSF using a generalized equation of a Gaussian. $G(x) = Ae^{\frac{-(x-\mu)^2}{2\sigma^2}} + O$, where A is the amplitude of the Gaussian, μ is the location, σ is the standard deviation, and O is the offset. Estimates of A, μ, σ and O represented as A_t, μ_t, σ_t and O_t, respectively are obtained from a least squares fit to obtain a model of the system LSF. Where t is the index of the single PEL width printed lines used to determine the LSF. This is represented in Eq. 2 as

$$S(A_t,\mu_t,\sigma_t,O_t) = \min\left\{\sum_{i=1}^{m}(LSF_i^t) - G^t(x_i)^2\right\} \qquad (2)$$

$S(A_t,\mu_t,\sigma_t,O_t)$ represents the experimental parameter set obtained from each 'm' samples of the LSF and its corresponding Gaussian fit (G) for every t single PEL width line. This set of t estimates was reduced to a mean parametric values $\hat{A}$, $\hat{\mu}$, $\hat{\sigma}$ and $\hat{O}$, for all line targets t. The mean estimated LSF curve is obtained as

$$LSFestimated = \hat{A}e^{\frac{-(x-\hat{\mu})^2}{2\hat{\sigma}^2}} + \hat{O}. \qquad (3)$$

Assuming the PSF is circularly symmetric, the mean LSF may be used to compute the 2-D PSF, with the LSF and 2-D PSF having the same standard deviation values. It should be noted that the printing system PSF approach is an approximation, since the printed PELs are discrete (i.e. impulses), located on the printer grid defined by the printer DPI, and not the continuous process of image data convolved with the PSF.

2-2-2 Optical Density Calculation

Traditional calculations of OD from the scanned data provide satisfactory density variations for Cyan, Magenta, and Black. However, it has been observed that OD variations for Yellow using traditional calculations are very "noisy" as shown Fig.4, resulting in inaccurate calibration results. To overcome this problem, opponent color substitutions for OD equations are used; in a manner similar to the methodology of computing dot gain based on opponent color substitutions in the Murray-Davies equation[4]. This modified OD calculation provides a solution that improves sensitivity to OD variations for Yellow as shown in Fig.4, while maintaining good detection of the variations for Cyan, Magenta and Black.

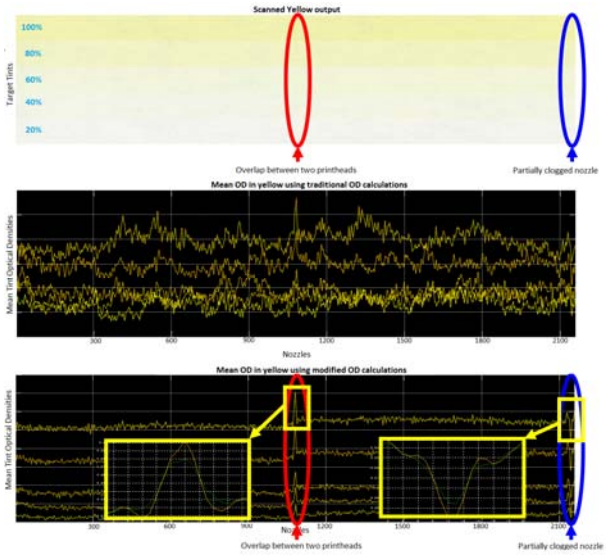

Fig.4 Mean OD in yellow using traditional OD and modified OD calculations.

Other measures, such as CIELab (L*) may also be employed. We used X, Y, and Z CIE tristimulus values for the OD values that were derived from the R, G, and B scanner values, which are assumed to be sRGB.

Traditionally, OD is defined as $OD = \log_{10}(\frac{100}{Y})$, where Y is "Luminance". RGB values were converted to CIE XYZ values using the equations given by Eq.4.

$$\begin{aligned} X &= 0.4124R + 0.3576G + 0.1805B \\ Y &= 0.2126R + 0.7152G + 0.0722B \\ Z &= 0.0193R + 0.1192G + 0.9505B \end{aligned} \quad (4)$$

Substituting for Y we have "new" OD equations $OD = \log_{10}(\frac{100}{X})$ for Cyan, $OD = \log_{10}(\frac{100}{Y})$ for Magenta and Black, and $OD = \log_{10}(\frac{100}{Z})$ for Yellow.

Using the estimated PSF and the OD values from the printed and scanned target, the OD values of each nozzle of the printing system are obtained using de-convolution. De-convolution is a solution to the inverse problem of estimating the effective input of a system, given the system output and PSF. This procedure increases the fidelity of the OD values, enabling more accurate estimates for non-uniformities by removing the blurring introduced by the printer and scanner.

The calibration module estimates the digital OD values for each tint on the target by assuming that the output $g(x,y)$ of the scanner is a 2-D convolution of the input $f(x,y)$ to the printing system, with the PSF $h(x,y)$. This can be expressed as $g(x,y) = f(x,y) ** h(x,y)$.

The Lucy Richardson de-convolution algorithm[5] was found to be most robust in our case of a known PSF. Following de-convolution, the image data for each printhead is resized to match the physical nozzle alignment for each printhead. This can be accomplished by scaling the scanned data to match the spacing between the measured single PEL width lines that are printed by known nozzles.

After scaling, the original OD values are estimated for each tint value from the step chart for each color. The differences between the mean OD values and the mean of the OD data set indicate the severity of the non-uniformity. Regions having abnormally large deviations from the mean represent areas with high non-uniformity.

2-3 Compensation

Module 3 generates calibrated 8-bit halftone screens based on the corrected OD values determined in Module 2. The compensation procedure involves generating a Transfer Function (TF) for each nozzle that maps the measured OD values to the desired OD of the pre-defined target. A high contrast sigmoidal shaped OD pre-defined target is used in this paper, since its functional shape is preferred by the Human Vision System (HVS). The calibrated halftone is created to achieve the same pre-defined target for each nozzle which reduces print non-uniformities caused by all three targeted mechanisms to a satisfactory level while also providing a consistent tonal response for the entire printhead array.

The flowchart in Fig.5 illustrates the process of compensating the print irregularities. Monotonicity is checked, to ensure mean OD increases with increasing gray levels to satisfy the requirement of a single valued inverse, required by the calibration. Clogged nozzles results in a rapidly decreasing mean OD spike, and a partially clogged nozzle results in deviated ink drop producing a negative OD transition adjacent to a positive transition in the mean OD. The calibration module ignores these full and partially clogged nozzles, replacing the data of the sheet image with the mean optical density of a neighboring nozzle for these malfunctions. This ensures that a reasonable value is used for this nozzle in the event that the nozzle begins to operate again, since these types of failures are transient. The calibration module linearly interpolates un-calibrated data and extrapolates as required, to generate 256 gray levels from a small number of measured gray levels in the printed sheet image. The calibration module uses a pre-defined target having a sigmoidal shape, using a relationship between gray levels (φ) and Optical Density (OD) defined as

$$OD_{target} = \begin{cases} OD_{\min} + \left\{ \left(\frac{\varphi}{128}\right)^{\gamma} * \frac{(OD_{\max} - OD_{\min})}{2} \right\} \\ for \quad 0 \le \varphi \ge 128 \\ OD_{\max} + \left\{ \left(255 - \frac{\varphi}{127}\right)^{\gamma} * \frac{(OD_{\max} - OD_{\min})}{2} \right\} \\ for \quad 128 \le \varphi \ge 255 \end{cases} \quad (5)$$

where γ is the exponential factor of the pre-defined target OD curve. Experimentally γ values of 1.2 produce pleasing HVS response. Linear OD is a sub case of sigmoidal, where the γ value is 1.0. The variables OD_{min} and OD_{max} are the minimum and maximum OD values derived from measured OD data. Based on the pre-defined target OD curve, the calibration module generates a transfer function on a per nozzle basis that maps the gray levels associated with measured OD values to gray levels associated with a sigmoidal target OD curve. $S_1 = T(r_1)$ is the measured OD curve and $S_2 = G(r_2)$ is the pre-defined target OD curve. The *TF* that maps S_1 to S_2 is expressed in Eq.6.

$$TF_{S_1 \to S_2} \Rightarrow T(r_1) = G(r_2) \Rightarrow r_1 = T^{-1}(G(r_2)) \quad (6)$$

Where r_1 and r_2 are the output and input gray levels respectively.

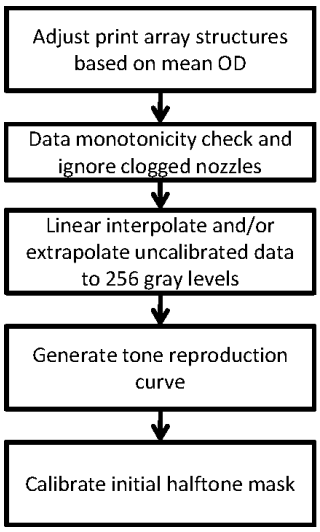

Fig.5 Compensation module flowchart.

3. Results

The proposed compensation algorithm is fully automated and does not require any human intervention. Qualitative results are illustrated in Fig.6 for Black. Figure 6 (a) is a scanned image showing printing from five printheads without any non-uniformity compensation and calibration. Figure 6 (b) is a scanned image of the same five printheads with the proposed non-uniformity compensation and calibration. Even though some small variations are visible in the Fig.6 (b), they were not visible by a human eye at the standard viewing distance. In the case where failures occurred, the root cause has been traced to a change in state of the printer from the time the input was obtained to the time when the output is printed, or variations in the paper transport such as web wandering, skew, etc. Space limitations prevent us from providing the quantitative results. The methodology permits any kind of paper, ink and print engine to be used. Our PSF characterization indicated sub-PEL consistency between various engines. A modified OD definition provided better compensation for Yellow and Cyan with increased sensitivity and de-convolution provided improved determination of the nozzle OD print values.

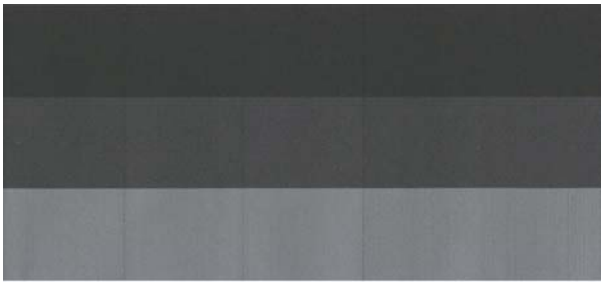

(a) Scanned image without compensation and calibration.

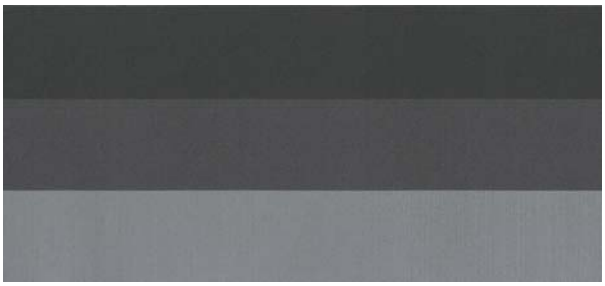

(b) Scanned output image of printer using proposed algorithm.

Fig.6 Final output with proposed calibration algorithm.

4. Conclusion

The proposed algorithm is aimed at providing a robust solution for compensating image non-uniformities 1) due to printhead overlap, 2) within each printhead, and 3) between printheads. The results obtained are "very encouraging", and demonstrate the potential of achieving improved image non-uniformity compensation. Challenges include geometric skew correction of the print data, compensation for clogged and partially clogged nozzles. Further improvements include creating a new test master design, improving the calibration algorithm by employing a spline interpolation scheme instead of linear interpolation, and improving the speed of computation for each transfer function.

References

1) M. Vans et al.: Automatic visual inspection and defect detection on variable data prints, *Journal of Electronic Imaging*, Vol.20, No.1 (2011).
2) K. Chandu, E. Saber, and W. Wu: A mutual information based automatic registration and analysis algorithm for defect identification in printed documents, *IEEE International Conference on Image Processing (ICIP)*, Vol.3, No.III, pp.449-452 (2007).
3) K. Chandu et al.: Direct multi-bit search (DMS) screen algorithm, *IEEE International Conference on Image Processing (ICIP)*, pp.817-820 (2012).
4) H. R. Kang: Digital Color Halftoning, SPIE-International Society for Optical Engineering (1999).
5) D. S. C. Biggs: Acceleration of iterative image restoration algorithms, *Applied Optics*, Vol.36, No.8, pp.1766-1775 (1997).